Variation Path Derivative of Travel-Time applied to Seismic Inversion

E. Contreras-Reyes [*] A. Osses, [†]

April 3, 2007

Abstract

Travel-time inversion requires the computation of the arrival time derivative with respect to some given parameter of the unknown medium, such as velocities or depth-nodes. We consider here two different types of travel-time inversion: (1) assuming that the final point of the ray-path is constant and (2) assuming that the initial angle of the ray-path is constant. When computing the travel-time derivative one get two main terms: one considers time variations along a constant ray-path in the perturbed medium (constant path derivative CPD) and the other one considers time variations owing to ray-path variation (variation path derivative VPD). Travel-time inversion of type (1) is the most widely used method in applications, and in this case VPD is commonly neglected as a second order term. Conversely, inversion of type (2) requires the explicit calculation of VPD as a first order term. We present here a comparative study between both inversion methods (1) and (2) in a simple one dimensional case by using a suitable exact expression for the travel-time derivative. Numerical tests in different situations show that inversion of type (2) behaves as an accurate inversion when considering both CPD and VPD. In addition, the explicit computation of the extra terms involved in VPD may be interesting for practical inverse nonlinear travel-time algorithms.

[*]IFM-GEOMAR, Leibniz-Institute of Marine Sciences, Wischhofstr. 1-3, 24148 Kiel, Germany (econtreras-reyes@ifm-geomar.de).

[†]Departamento de Ingeniería Matemática, Facultad de Ciencias de Físicas y Matemáticas, Universidad de Chile, Casilla 170/3 - Correo 3, Santiago, Chile y Centro de Modelamiento Matemático, UMR 2071 CNRS-Uchile (axosses@dim.uchile.cl). This work has been partially supported by FONDECYT 1061263 and SAEMC-IAI and TIC-AMSUD-Conicyt grants.

1 Introduction

The complexity of travel-time inversion requires the efficient computation of time derivatives with respect to some given parameter of the unknown medium. The model parameters might be velocity nodes, position of boundary nodes, velocity gradients, etc. These parameters define the medium and the corresponding velocity-structure. Let $\mathbf{m} = (m_1, m_2, ..., m_M)$ be the vector of M parameters and let $\mathbf{t} = (t_1(\mathbf{m}), t_2(\mathbf{m}), ..., t_N(\mathbf{m}))$ be the travel-time vector, where N is the number of available time-data.

The time derivative $\frac{\partial t_i}{\partial m_j}$ involves two main terms: the first considers time variations related to parameter variation along the original ray-path (constant path derivative CPD). The other term considers time changes due to the variation of the original path (variation path derivative VPD). We consider here two different types of time derivative, which are adapted for two different types of inversion: (a) assuming that the final point of the ray-path x_r^i remains constant and (b) assuming that the initial angle of the ray-path θ_0^i remains constant. That is to say

$$(1)\ \left.\frac{\partial t_i}{\partial m_j}\right|_{x_r^i=ct.} \qquad (2)\ \left.\frac{\partial t_i}{\partial m_j}\right|_{\theta_0^i=ct.}$$

Travel-time inversion of type (1) is the most commonly used method and in this case VPD is usually neglected as a second order term (see Aki, Richards, 1990 [1], Snieder, Sambridge, 1993 [8]). This type of inversion corresponds to match observed and modeled time at the same arrival point. Inversion of type (2) requires the explicit calculation of VPD, and the comparison between observed and predicted arrival time are done for the same initial angle. Figure 1 shows schematically the two types of inversion.

In the following sections we introduce the computation of the travel-time derivative and its application for the inverse problem for the 1D velocity depth distribution. We compare the velocity of convergence between both types of inversion (1) and (2). In the appendix, we summarize by means of an 2D example, some basic ideas about one of the most widely used numerical methods in travel-time inversion: the minimization of a penalized and weighted cost functional using a quasi-Newton inversion scheme.

2 Constant and variation path derivative of the travel-time

Let t_i be the $i-th$ travel-time between a source located at (x_0, z_0) and a receptor (x_r, z_r) along the ray-path $\gamma_i(x_0, z_0)$ (geodesic) in a continuous medium with velocity field $V(\vec{x})$, $\vec{x} = (x, z)$.

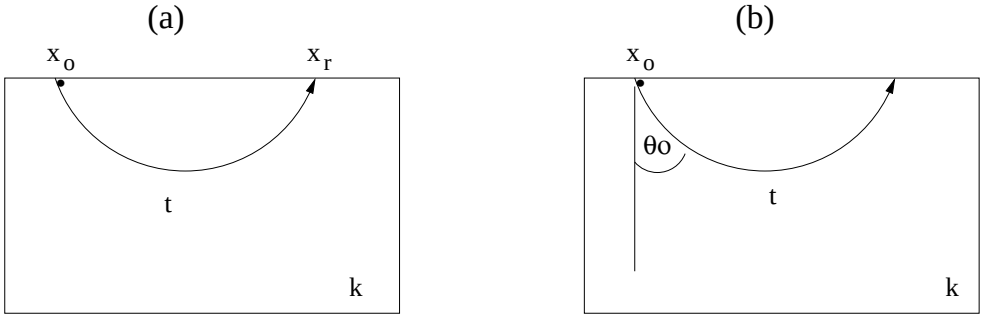

Figure 1: Schematic illustration of the two different kind of inverse problems. The velocity gradient k is unknown and can be estimated knowing either **left:** (a) the initial and final points of the ray-path and travel-time $((x_0, x_r, t))$, or **right:** (b) the initial point and angle of the ray-path and travel-time $((x_0, \theta_0, t))$.

The travel-time t_i is given in the integral form as follow

$$t_i = \int_{\gamma_i} \frac{ds}{V(x(s), z(s))} \tag{1}$$

In the case of inversion of type (1), γ_i is uniquely determined by the location of the receiver x_r^i, and in the case of inversion of type (2) γ_i is determined by the initial angle θ_0^i. The velocity distribution is a function of parameters m_j, i.e $V = V(\vec{x}, m_1, \ldots, m_M)$. The partial derivative of the $i-th$ travel-time t_i with respect to the parameter m_j is given by (see a more general formula in the Appendix):

$$\frac{\partial t_i}{\partial m_j} = -\int_{\gamma_i} \frac{1}{V^2}\frac{\partial V}{\partial m_j}\, ds + \left.\frac{\vec{u}\cdot\hat{s}}{V}\right|_{(x_r,z_r)} + \int_{\gamma_i}\left(\frac{\kappa}{V} - \frac{1}{V^2}\nabla V\cdot\hat{n}\right)(\vec{u}\cdot\hat{n})\, ds, \tag{2}$$

where $\hat{n}$, $\hat{s}$ are the unit normal and tangent vectors of the ray-trajectory in a bidimensional medium (following the sense of the parametrization of γ), κ is the curvature, and $\vec{u}$ represents the velocity of the ray-trajectory due to the variation of the parameter m_j (see Figure 2).

The first term on the left-hand side of (2) represents the derivative of the time not including the variation of the ray-trajectory, i.e approximation of the first order see e.g Aki, Richards, 1980 [1]. We refer to this first terms as *Constant Path Derivative* or CPD.

The other terms on the right-hand side of (2) correspond to the derivative of the time due to the variation of the ray-trajectory (the first one among them is evaluated at the final point of the trajectory (x_r, z_r)). See Snieder, Sambridge, 1993 [8] for some particular parametrizations

where these terms are considered. We refer to these part of the derivative (second and third terms in 2) as the *Variation Path Derivative* or VPD.

In order to explain the geometrical interpretation of $\vec{u}$ in the formula (2), let us consider a ray-trajectory γ corresponding to a value m_j of the parameter, and a second perturbed trajectory $\gamma + \delta\gamma$ corresponding to a perturbed parameter $m_j + \delta m_j$. Every point (x, z) on γ has a new position $(x + \delta x, z + \delta z)$ on the new trajectory $\gamma + \delta\gamma$ corresponding to the same angle θ. The limit vector field $\frac{1}{\delta m_j}(\delta x, \delta z)$ as δm_j tends to zero is $\vec{u}$. Thus, consequently $\vec{u}$ is referred as the velocity of the trajectory with respect to the parameter m_j.

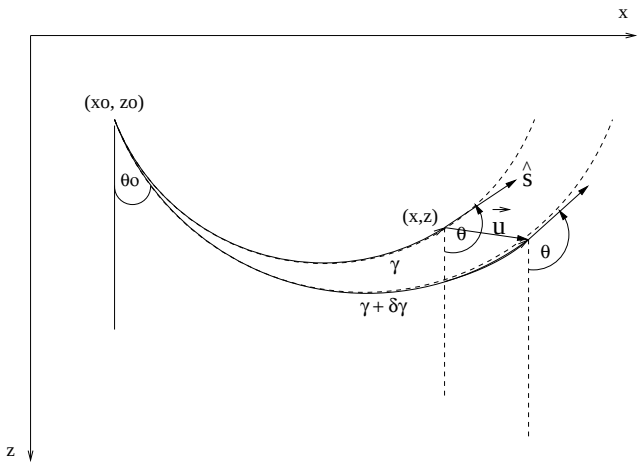

Figure 2: Representation of the variability of the ray-path owing to a variation of the parameter m_j. The source is located at (x_0, z_0), with constant initial angle θ_0. The tangent vector of the ray-path is $\hat{s} = (\sin\theta, \cos\theta)$. The vector field $\vec{u} = \left(\frac{\partial x}{\partial m_j}, \frac{\partial z}{\partial m_j}\right)$ represents the velocity of the ray-trajectory.

3 Application to a 1D linear velocity-depth distribution

In several geological settings the 1D lineal velocity-depth distribution responds quite well to model geological layers of the Earth. In this case, the forward problem has an analytical solution, see e.g Červený et al., 1977 [3] or Aki, Richards 1980 [1] among others. The velocity field is linear and depends only on the depth i.e $V(z) = v_0 + k \cdot (z - z_0)$, where $k = \frac{v_L - v_0}{z_L - z_0}$ is the vertical constant gradient, v_t and v_b are the velocities at the top $z = z_0$ and the bottom $z = z_b$

respectively (Figure 3). The vertical gradient is a function of the parameters, which define the model $k = k(m_j)$. Some useful known expressions are:

$$(x, z) = \left(x_0 + R(\cos\theta_0 - \cos\theta), z_0 - R(\sin\theta - \sin\theta_0) \right), \; R = \frac{1}{kp}, \; p = \frac{\sin\theta_0}{v_0} \tag{3a}$$

$$t = \frac{1}{k} \cdot \ln\left(\frac{\tan(\theta/2)}{\tan(\theta_0/2)} \right) \tag{3b}$$

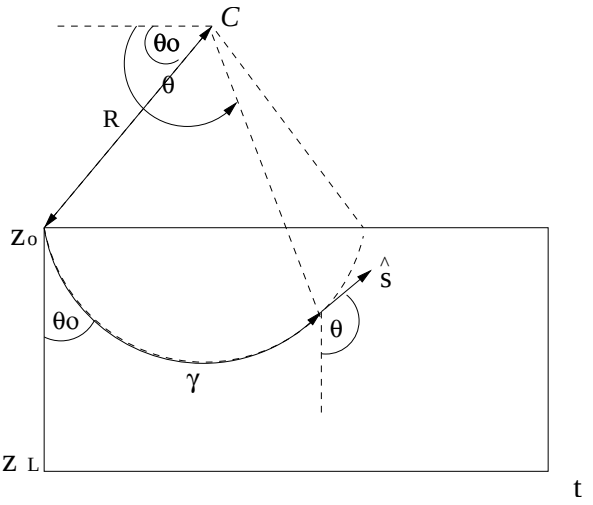

Figure 3: Representation of velocity field with a constant velocity gradient. The ray-path is circular and the radius is given by $R = 1/kp$, with center located at $C = (z_0 - R\sin\theta_0, x_0 + R\cos\theta_0)$.

We choose the angle θ to parametrize the ray-path γ (see Figure 3). With this parametrization, the unit normal and tangent vectors of the ray-path are given by

$$\hat{n} = (-\cos\theta, \sin\theta), \quad \hat{s} = (\sin\theta, \cos\theta). \tag{4}$$

Using equation 3a and 3b, we can calculate analytically CPD and VPD_1, VPD_2, which are respectively the first, second and third terms of equation 2. Indeed

$$CPD = -\int_{\theta_0}^{\theta} \frac{1}{V^2}\frac{\partial V}{\partial m_j} \cdot ds = -\frac{\partial k}{\partial m_j}\frac{1}{k^2}\left[\ln\left(\frac{\tan(\theta/2)}{\tan(\theta_0/2)} \right) + \sin\theta_0(\operatorname{cotan}\theta - \operatorname{cotan}\theta_0) \right] \tag{5}$$

$$VPD_1 = \left.\frac{\vec{u}\cdot\hat{s}}{V}\right|_{(x(\theta),z(\theta))} = -\frac{\partial k}{\partial m_j}\frac{v_0\cdot\sin(\theta-\theta_0)}{k^2\,V\,\sin\theta_0} \tag{6}$$

$$VPD_2 = \int_\gamma \left(\frac{\kappa}{V} - \frac{1}{V^2}\nabla V\cdot\hat{n}\right)(\vec{u}\cdot\hat{n})\,ds = \int_\gamma \left(\frac{1}{R}\frac{\sin\theta_0}{v_0\sin\theta} - \left(\frac{\sin\theta_0}{v_0\sin\theta}\right)^2 k\sin\theta\right)(\vec{u}\cdot\hat{n})\,ds = 0, \tag{7}$$

where we have used that $\kappa = 1/R$ and $\nabla V = k\hat{z}$. Notice that it is not necessary to compute $\vec{u}\cdot\hat{n}$, but it is not difficult to give its exact expression in this case:

$$\vec{u}\cdot\hat{n} = -\frac{\partial k}{\partial m_j}\frac{v_0(1-\cos(\theta-\theta_0))}{k^2\sin\theta_0}. \tag{8}$$

It is then straightforward to verify that

$$\frac{\partial t}{\partial m_j} = CPD + VPD_1 + VPD_2 = -\frac{\partial k}{\partial m_j}\frac{1}{k^2}\ln\Big(\frac{\tan(\theta/2)}{\tan(\theta_0/2)}\Big), \tag{9}$$

which is the same result obtained after taking directly the derivative in the expression given by 3b with with respect to the parameter m_j.

4 Inversion of the velocity gradient

We present an example of the inversion of the constant velocity gradient $\bar{k}$, using inversion of type (1) and (2) by observing the travel-time of refracted waves along a single layer (Figure 4). Taking v_t=4.0 km/s, v_b=6.5 km/s, z_0=0 km and z_b=2 km, this layer represent a typical Layer 2 for oceanic crust (e.g White, 1992 [10]). To construct the synthetic data set, we use equation 3b. Since the arrival rays arrive at an angle of $\theta = \pi - \theta_0$ at the top of the layer (see Figure 4), then the arrival times are given by

$$\bar{t} = -\frac{2}{k}\ln(\tan(\theta_0/2)). \tag{10}$$

We can also compute the x-position of the arriving rays at the top of the layer, using the horizontal component of 3a. The location of the arriving refracted waves are given by,

$$\bar{x} = x_0 + \frac{2\cos\theta_0}{kp}. \tag{11}$$

Using the velocity and depth values mentioned above, we construct a set $(\bar{x},\bar{t})$, for refracted waves from $\theta_0 = \theta_c$ to π, where θ_c is the critic angle where the refracted wave starts and given by $\theta_c = \arcsin(v_t/v_b)$. We use an increment of $\delta\theta_0 = 5 * \pi/180$. Figure 4 shows the ray-tracing associated to the synthetic travel-times for the refracted wave explained above.

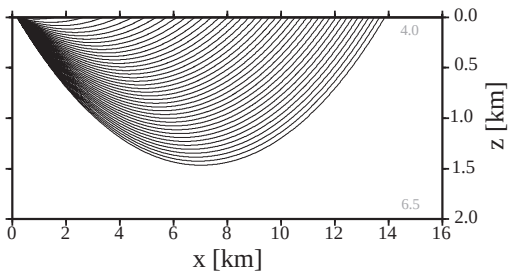

Figure 4: The seismic source is located at $(x_0, z_0) = (0, 0)$ and the initial angle is taken in the range $\arcsin(v_t/v_b) \sim 0.21\pi$ to π. The velocity gradient is 1.25 s^{-1}. The gray numbers at the top and bottom of the layers are the used P-wave velocities values.

4.1 Inversion of Type 1

In this case the x-locations of the arrivals waves are know and the initial angles unknown (this case corresponds to the most realistic case). Let be (x, t) our predicted travel-times, the idea is to find $\hat{k}$ such that $t(\hat{k}) = \bar{t}$. Let be k_0 the starting velocity gradient, thus $t_0 = t(k_0)$, as we know x we use equation (11) assuming $x_0 = 0$ for simplycity,

$$\bar{x} = \frac{2\cos\theta_0}{k_0 p} = \frac{2v_t}{k_0 \tan\theta_0} \tag{12}$$

Thus, we get the initial angles which allow the arrivals waves of the starting models arrive exactly at the locations x.

$$\theta(k_0) = \arctan\left(\frac{2v_t}{k_0\hat{x}}\right) \tag{13}$$

Taking (10) we get k iteratively by

$$k_{n+1} = \frac{-2\ln(\tan(\theta_0(k_n)/2))}{\bar{t}} \tag{14}$$

Notice that in this case $VPD_1 = 0$ since $\hat{s}(x_r, z_r) = 0$ and $VPD_2 = 0$ with the same calculation of formula 7.

Figure 5, left hand side shows the convergence of k_n for different starting velocity gradients (k_0 = 0.5,1.0,2.0,3.0 s^{-1}) with stopping criterion $|k_{n+1} - k_n| < 0.01$ s^{-1}. For starting values further than the real model ($k = 1.25s^{-1}$), the method needs a greater number of iterations. The method is very robust and efficient for large starting velocity gradients. We interpret this as the better ray-coverage through the model, due to deeper penetration of the rays associated to the high velocity gradient. For smaller starting values of k_0 the pseudo-inversion method needs a greater number of iterations.

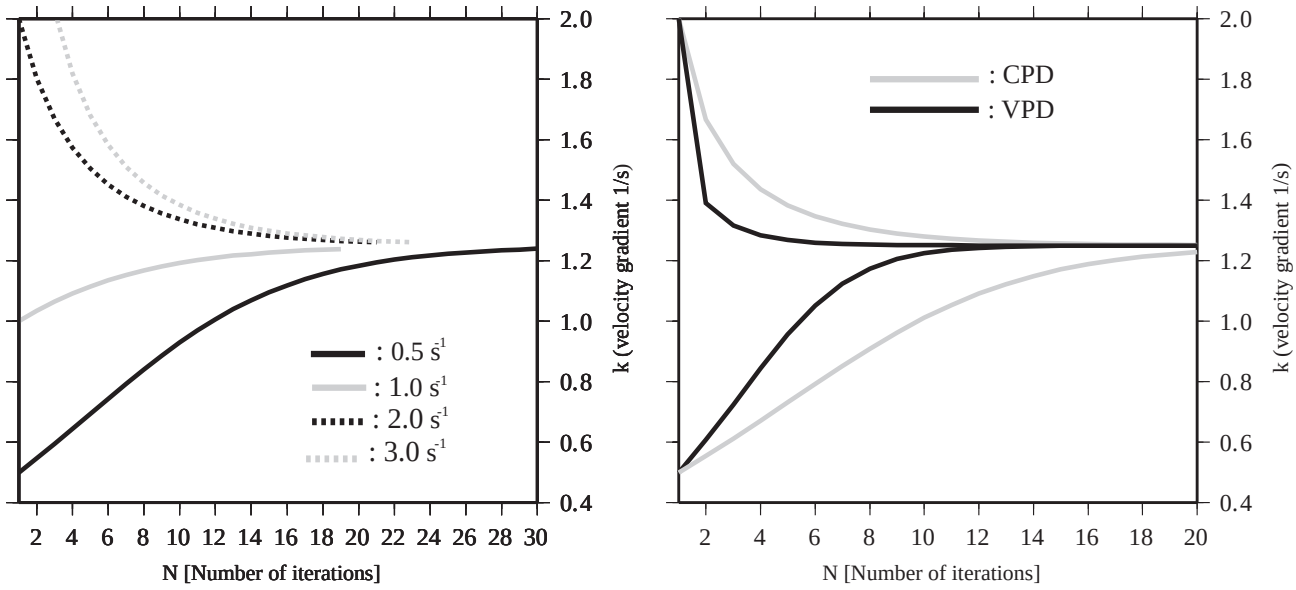

Figure 5: **Left**: study of the relative error of parameter k as a function of the number of iterations for inversion of type (1) and for different starting models corresponding to $k_0 = 0.5$, 1.0, 2.0 and 3.0 s^{-1}. **Right**: Study of the relative error of parameter k as the number of iterations for the inversion of type (2). CPD and VPD velocity of convergence are compared for two starting models corresponding to $k_0 = 0.5$ and $k_0 = 2.0$ s^{-1} respectively. The iterative methods are stopped when $|k_{n+1} - k_n| < 0.01$ s^{-1}.

4.2 Inversion of Type 2

This case is quite straightforward, since we know the initial angle θ_0. We have just to invert equation 3b without the need to use neither a starting model nor an iterative approach. The corresponding linear system is solved by a least square method. The solution is expressed by $\hat{k} = -\frac{2}{t}\ln(\tan(\theta_0/2))$

4.3 Comparison using a quasi-Newton method

In order to apply the derivative of the travel-time related to the velocity gradient, we employed a quasi-Newton method (see Appendix). We compare derivative of Inversion type (1) and (2), using the same starting model. Firstly, we compute the analytical derivative related to k for both cases.

(Case 1) We have to calculate $\frac{\partial t_i}{\partial m_j}\Big|_{x_r^i=ct}$. Here, $VPD = VPD_1 + VPD_2$ vanishes and

$$\frac{\partial t_i}{\partial m_j}\Big|_{x_r^i=ct} = -\frac{1}{k^2}\Big[-2\ln(\tan(\theta/2)) + \sin\theta\cdot(\tan\theta_0 - \operatorname{cotan}\theta_0)\Big]$$

(Case 2) for inversion of type (2), we have to know $\frac{\partial t_i}{\partial m_j}\Big|_{\theta_0^i=ct}$, which is $\frac{\partial t_i}{\partial m_j}\Big|_{\theta_0^i=ct} = -\frac{2}{k^2}\ln(\tan(\theta_0/2))$.

The convergence of the parameter k is studied, using both type of derivatives. Figure 5 right, shows the behaviour of the convergence for CPD and VPD, both starting with the same initial velocity gradient k_0 of 0.5 and 2 s^{-1}. VPD converges faster and more efficient for both starting cases to the true vertical velocity gradient $\bar{k}$=1.25 s^{-1}.

The tests studied above show the efficiency of the second term VPD. However, we have been using only one parameter in our simplified model (the velocity gradient). In several geological setting, such as subduction zones, spreading centres or hotspot areas the velocity distribution is far of being one dimensional. A further approach should incorporated several parameters in the velocity model.

5 Conclusions

Two different types of inversion have been studied here, (1) assuming that the final point of the ray-path remains fixed and (2) assuming that the initial angle of the ray-path remains unchanged. Inversion of type (2) converges quickly and more efficiently than inversion of type (1), independently of the initial models used. Nevertheless, inversion of type (2) requires the knowledge of the initial angle of every ray, whose source control is unrealistic. However, an equivalent parametrization of the seismic rays could improve the method in order to use the variation of the ray-path.

6 Appendix

6.1 Derivative of surface integrals

Let $\gamma(t) = \gamma_0 + t\vec{u}$ be a family of smooth manifolds in $\mathbb{R}^n$ of co-dimension 1 (lines in $\mathbb{R}^2$ or surfaces in $\mathbb{R}^3$) perturbed from the reference manifold γ_0 and with area element $d\sigma$. Let $\hat{n}$ and $\hat{s}$ be respectively the unit normal and tangent vectors of γ_0 following the sense of its parametrization. Let κ be the main curvature of the manifold. Given a smooth function $F(t)$ defined in a neighborhood in $\mathbb{R}^n$ of γ_0, we have

$$\frac{d}{dt}\int_{\gamma(t)} F(t)\,d\sigma = \int_{\gamma_0} \frac{\partial F}{\partial t}\,d\sigma + \int_{\gamma_0} \operatorname{div}(F\vec{u}_{\hat{s}})\,d\sigma + \int_{\gamma_0} (\nabla F\cdot\hat{n} + (n-1)\kappa F)\,(\vec{u}\cdot\hat{n})\,d\sigma$$

where div stands for the surface divergence if $n = 3$ or the tangent derivative if $n = 2$. If γ_0 has no boundary or if the tangent component of the velocity of the perturbation $\vec{u}_{\hat{s}} = \vec{u} - (\vec{u}\cdot\hat{n})\hat{n}$ vanishes on γ_0 then the second integral term in the formula above is zero. The formula is deduced as for transport theorems writing the integral on the reference manifold before taking the derivative (see for instance Meyer, 1982 [5]).

6.2 2D ray-tracing

The first-order ordinary differential system of the 2D ray-tracing comes from the high frequency approximation of the wave equation (Eikonal's equation). Alternatively these equations can be obtained using the Fermat's principle. The system is non-linear and allows the calculation of the trajectory and the arrival time of the ray.

Let z be the depth and x be the horizontal variable and let $V(x, z)$ be the wave velocity in a bidimensional and inhomogeneous medium. The variable θ is the angle between the tangent to the ray and the vertical axis oriented counter clockwise. The 2D ray-tracing equations are (e.g., Červený et al., 1977 [3]):

$$\frac{dx}{dt} = V(x,z)\cdot\sin\theta \tag{15a}$$

$$\frac{dz}{dt} = V(x,z)\cdot\cos\theta \tag{15b}$$

$$\frac{d\theta}{dt} = -\frac{\partial V}{\partial x}\cdot\cos\theta + \frac{\partial V}{\partial z}\cdot\sin\theta \tag{15c}$$

$$-\pi \le \theta \le \pi$$

In practice, within a continuous medium, a Runge-Kutta method of fourth order with error control can be used to solve for x, z and θ (Sherriff and Geldart, 1983) [7]. Snell's law (involving refraction and reflection) is applied at discontinuities in the medium.

6.3 Travel-time inversion and quasi-Newton method

For a systematic presentation of quasi-Newton and other general minimization methods applied to seismic traveltime inverse problems see e.g. Rawlinston, Sambridge, 2003 [6] or Tarantola, 1987 [9].

Let be $t(\mathbf{m})$ the time predicted through the solving of the ray-tracing (see previous subsection), for a given model $\mathbf{m}$. The time predicted values cannot, in general, be identical to the true "time-observed" ($\bar{t}$), due to modelling errors and experimental uncertainties. Let be C_t the estimated data and model covariance matrix, which represents the uncertainties of the phase arrival picking error and the data noisy. Also, there are uncertainties of the model parameters associated to the deviation and error propagation, let be C_m the covariance matrix. The inverse problem consists of obtaining an effective method of minimization of the functional:

$$\psi(\mathbf{m}) = \frac{1}{2} \cdot [t(\mathbf{m}) - \overline{\mathbf{t}}, C_t^{-1} \cdot g(\mathbf{m}) - \overline{\mathbf{t}}] + \frac{1}{2} \cdot [\mathbf{m} - \mathbf{m_0}, C_m^{-1} \cdot (\mathbf{m} - \mathbf{m_0})] \tag{16}$$

Where m_0 is the initial model. (11) represenst the functional to minimize, the gradient of the ψ is given by:

$$\nabla J(\mathbf{m}) = G^t \cdot C_t^{-1} \cdot (g(\mathbf{m}) - \overline{\mathbf{d}}) + C_m^{-1} \cdot (\mathbf{m} - \mathbf{m_0}) \tag{17}$$

Where $G_{ij} = \frac{\partial t_i}{\partial m_j}$ is partial derivatives matrix, with dimension NxM where N is the number of data and M the number of model parameters. This matrix is obtained calculated analytically using equation (2) during the ray-trace for those model parameters selected for adjustment.

Following the Quasi-Newton algorithm presented by Tarantola, 1987 [9], the parameters are estimated iteratively by:

$$m_{k+1} = m_k - \mu_k \cdot \widehat{H}_k^{-1} \cdot \widehat{\gamma_k} \tag{18}$$

where $\widehat{H}_n$ is the Hessian of ψ, which in approximated form is given by $\widehat{H}_k = G_k^t \cdot C_t^{-1} \cdot G_k + C_m^{-1}$

The gradient of ψ evaluated at m_k, is given by $\nabla J(\mathbf{m}_k) = G_k^t \cdot C_t^{-1} \cdot (t(m_k) - \overline{d}) + C_m^{-1} \cdot (m_k - m_0)$

The optimum value for μ_k has to be obtained by linear search. A linearization of $t(m)$ around $g(m_k)$ gives $\mu_k \sim 1$. However, for nonlinear problems, this approximation may not be adequate, and a more elaborate linear search along the Newton direction has to be made e.g. Tarantola, 1987 [9].

6.4 Numerical example of quasi-Newton method to 2D travel-time inversion

In order to explain the basic ingredients of the numerical algorithms used in travel-time inversion, let us develop a simple example of numerical travel-time inversion.

6.4.1 Model Parameterization

We employed at trapezoidal parameterization suggested by Zelt and Smith (1992), a layered and variable-block-size representation of 2-D isotropic velocity structure. For a model trapezoid, has four corner spatial coordinates and velocities, represented by two points on the top $P_{1a} = (x_1, z_1a, v_{1a})$ and $P_{2a} = (x_2, z_2a, v_{2a})$. And two points on the bottom $P_{1b} = (x_1, z_1b, v_{1b})$ and $P_{2b} = (x_2, z_2b, v_{2b})$. Thus way, the four boundaries are $x = x_1$, $x = x_2$, $z_a(x) = z_{1a} + \frac{\Delta z_a}{\Delta x} \cdot (x - x_1)$ and $z_b(x) = z_{1b} + \frac{\Delta z_b}{\Delta x} \cdot (x - x_1)$, where $\frac{\Delta z_a}{\Delta x} = \frac{z_{2a} - z_{1a}}{\Delta x_2 - x_1}$ and $\frac{\Delta z_b}{\Delta x} = \frac{z_{2b} - z_{1b}}{\Delta x_2 - x_1}$. Similarly, the velocity along the top and bottom border is $v_a(x) = v_{1a} + \frac{\Delta v_a}{\Delta x} \cdot (x - x_1)$ and $v_b(x) = v_{1b} + \frac{\Delta v_b}{\Delta x} \cdot (x - x_1)$ respectivaly. Where $\frac{\Delta v_a}{\Delta x} = \frac{v_{2a} - v_{1a}}{\Delta x}$ and $\frac{\Delta v_b}{\Delta x} = \frac{v_{2b} - v_{1b}}{\Delta x}$ (see fig 4).

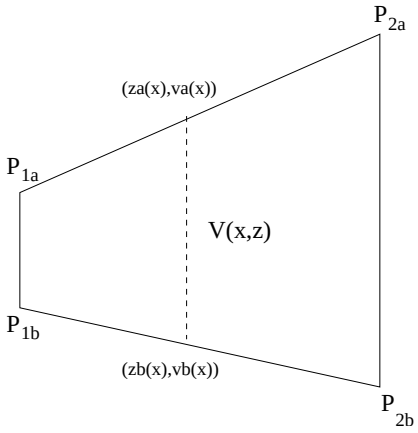

Figure 6: The continuous field velocity $V(x, z)$ is defined by the four nodes P_{1a}, P_{2a}, P_{1b} and P_{2b} (see text for details).

For a given x, by interpolating the velocity $V(x, z)$ between the points $(z_a(x), v_a(x))$ and $(z_b(x), v_b(x))$ (Figure 6), we obtain:

$$V(x, z) = v_a + \frac{dV}{dz} \cdot (z - z_a(x)), \quad \frac{dV}{dz} = \frac{v_b(x) - v_a(x)}{z_b(x) - z_a(x)} \tag{19}$$

where $\frac{dV}{dz}$ is the vertical velocity gradient. For construction, $V(x,z)$ is non-linear inside of the trapezoid, but it is a linear function of z for a fixed x.

In order to approximate the geometrical derivate for each ray as a function of the initial and final incident angle, we have to take some representative values of v_L, z_o and z_L. This values can be obtained as follows: (1) k can be estimated as the mean value of the vertical gradient for the extremes of the trapezoid, i.e $\bar{k} = \frac{(\frac{(v_L - v_0)}{(z_{2b} - z_{2a})} + \frac{(v_L - v_0)}{(z_{1b} - z_{1a})}}{2}$, (2) if $(\tilde{x}, \tilde{z})$ is the arrival point for the ray, we can also do the following approximation: $\bar{z_L}(x) = \frac{z_{1b} - z_{1a} + z_b(x) - z_a(x)}{2}$, (3) and finally, we can obtain the value of v_L by $v_L = \bar{k} \cdot \bar{z_L}(x) + v_0$.

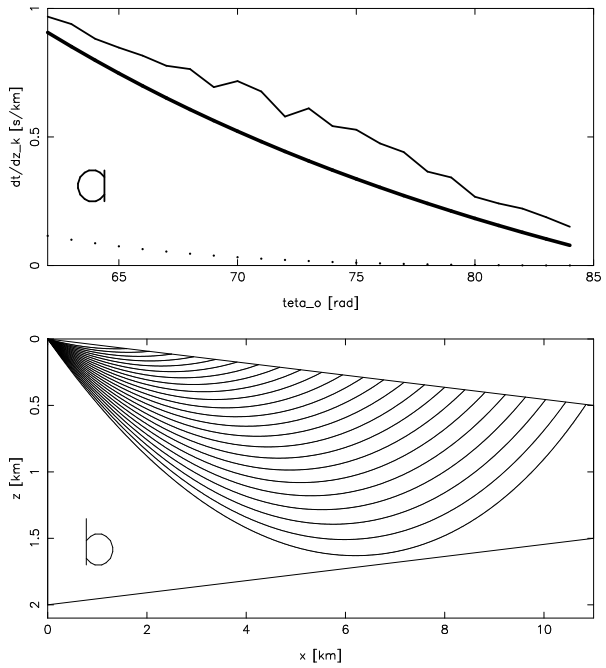

Figure 7: Example of refracted waves, with a source located at the origin. **Up:** the rays are fired with initial angles θ_o : 61^o to 85^o as shown in (b). **Down:** in figure (a), the thin line represents the numerical derivate taken with respect to the boundary depth ($\frac{\partial t}{\partial z_L}$). The bold line is the calculated VPD, which has a maximum at 61^o, angle associated to the longest ray through the trapezoid. The numerical values are: z_{1a}=0 km, z_{1b}=2.0 km, z_{2a}=0.5 km, z_{2b}=1.5 km, $v_{1a} = v_{2a}$ =5.0 km/s, $v_{1b} = v_{2b}$ = 6.5 km/s.

6.4.2 Test using synthetic data

To study the convergence of the parameters, we present a synthetic velocity model and traveltimes typical of a wide-angle seismic experiment. This model is compressed by four layers: water (1.5 km/s), upper crust ($3.3 - 5.0$ km/s), lower crust ($6.5 - 7.0$ km/s) and upper mantle ($8.0 - 8.22$ km/s). In order to symplify the test, the velocities at the nodes are fixed, and the only parameters to be recovered are those linked to the geometry of the Moho, defined by six depth boundaries. We point out that these parameters have only one degree of freedom, since they are restricted to move vertically. The length of the model is 200 km with strong variability of the interface geometry (Figure 8). During the inversion, we have only used two seismic sources located on the sea-floor (using the principle of reciprocity) (Figure 9).

The Moho reflector is usually better constrained by inverting refracted and reflected arrivals in the oceanic crust. Here, however, we only used refracted arrivals in the upper mantle (P_n) to invert the reflector in order to study the resolvity of those arrivals. We carried out two tests: one with noise-free data and another one with a Normal distribution of noise data, with a covarience of $+/-0.1s$. For both sets of data, the following matrixes of covariance were used: $C_t = \text{diag}\{+/-0.01s\}$ and $C_m = \text{diag}\{1km\}$ taken from (Zelt and Smith, 1992).

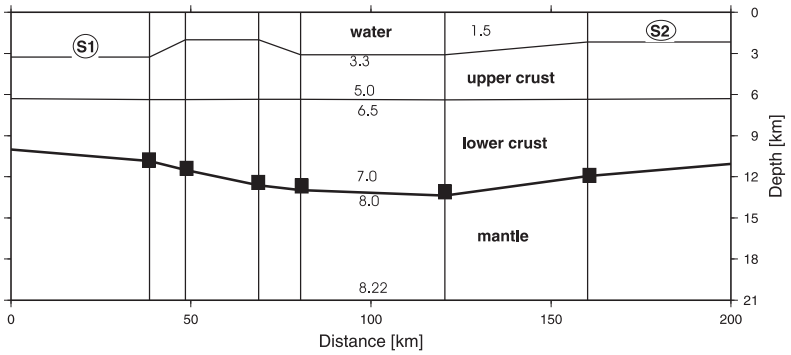

Figure 8: True synthetic model is compressed by four layers. Typical velocities of water, upper crust, lower crust and upper mantle were used, and they were retained fixed during the inversion. The parameters to invert are the six boundary nodes (solid squares), which defined the geometry of the Moho interface.

The initial model of the geometry is a simple horizontal line, where each depth boundaries is constant equal to 10.85 km (Figure 10a). The RMS of the parameters is showed at Figure 10b.

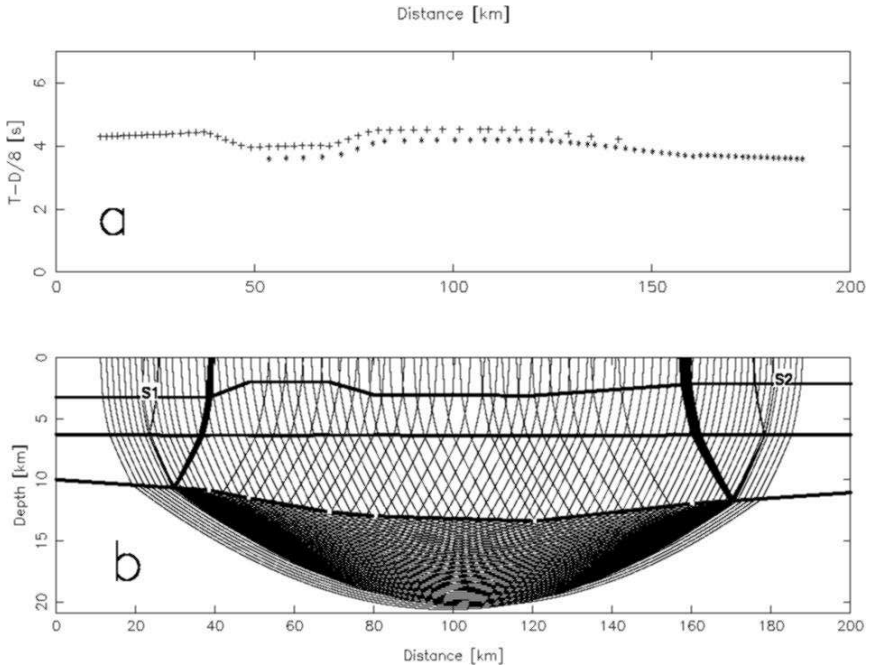

Figure 9: Synthetic travel-timed (a) based on model showed in Figure 8, using 2 seismic sources (S1 and S2). Corresponding raytracing of uppermost mantle phases (b).

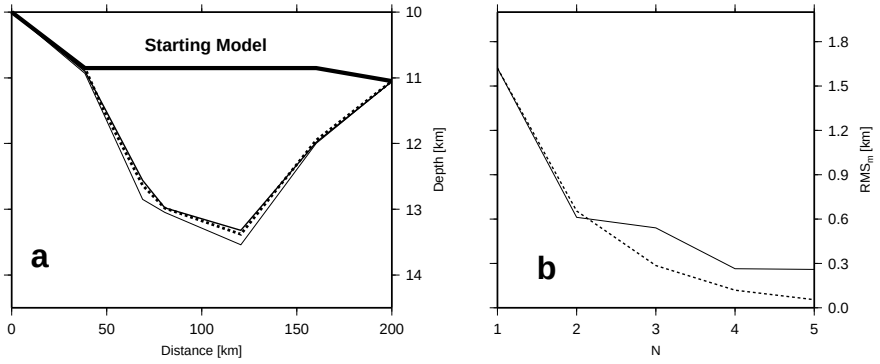

Figure 10: (a) The solid line SM represents the Starting Model for the geometry of seismic interface Moho. Only a slight difference exists between the true model TM and the estimated model with free data noise FDN (dashed line). The estimated model with data noise DN is represented by the thinner line. (b) RMS of the parameters with free data noise (dashed line) and data noise (solid line).

Acknowledgments

This work was started during a research stay of the first author at the Centro de Modelamiento Matemático, UMI 2807 CNRS-Uchile, Universidad de Chile, Santiago, Chile. The authors acknowledge the support of this Center for financing this interdisciplinary research. The authors also acknowledge the informatics support of data assimilation labs related to SAEMC-IAI and TIC-AMSUD projects and Prof. Emilio Vera at the Geophysical Department of the University of Chile for providing the real data and supervision. We also gratefully acknowledges a scholarship granted by the German Academic exchange Service (DAAD) to the first author.

References

[1] Aki K. and Richards P.G., 1980. *Quantitative Seismology*, vol. 1-2, Freeman, San Francisco.

[2] Luetgert J., 1992. MacRay-Interactive two-dimensional seismic ray-tracing for the Macintosh. USGS Open file Rept, 92–356.

[3] Červený V., Molotkov I. and Pšenčík I., 1977. *Ray Method in Seismology*. University of Karlova, Prague, Chzechoslovakia.

[4] Korenaga J., Holbrook W.S., Kent G.M, Kelemen P.B., Detrik R.S., Larsen H.-C., Hopper J.R. and Dahl-JensenT., 2000. Crustal structure of the southeast Greenland margin from joint refraction and reflection seismic tomography, *J. Geophys. Res.*, **105** 21, 591-21, 614.

[5] Meyer R.E., 1982. *Introduction to Mathematical Fluid Dynamics*, Dover.

[6] Rawlinson N. and Sambridge M., 2003. Seismic traveltime tomography of the crust and lithosphere, *Advances in Geophysics*, **46**, 81–198.

[7] Sheriff R.E. and Geldart L.P., 1983. *Exploration Seismology, vol.2: Data Proccesing and Interpretation*, Cambridge Univerisity Press, Cambridge, UK.

[8] Snieder R. and Sambridge M., 1993. The ambiguity in ray perturbation theory. *J. Geophys. Res.*, **98**, 22021–22034.

[9] Tarantola A., 1987. *Inverse Problem Theory*, Elsevier, Amsterdam.

[10] White R. S., McKenzie D., O'Nions R. K., 1992. Oceanic crustal thickness from seismic measurements and rare earth element inversions, *J. Geophys. Res.*, **97**, 19683-19715.

[11] Zelt C.A. and Ellis R.M., 1988. Practical and efficent ray-tracing in two-dimensional media for rapid travel-time and amplitude forward modelling, *Can. J. Explor. Geophys.*, **24**, 16–34.

[12] Zelt C.A. and Smith R.B., 1992. Seismic travel-time inversion for 2-D crustal velocity structure. Geophys. J. Int., **108**, 16–34.